Electronic Supplementary Material (ESI) for Materials Chemistry Frontiers.

Highly Selective Removal of Heterocyclic Impurities from Toluene by Nonporous Adaptive Crystals of Perethylated Pillar[6]arene

Weijie Zhu, Errui Li, Jiong Zhou, Yujuan Zhou, Xinru Sheng, and Feihe Huang*

State Key Laboratory of Chemical Engineering, Center for Chemistry of High-Performance & Novel Materials, Department of Chemistry, Zhejiang University, Hangzhou 310027, P. R. China. Fax and Tel: +86-571-8795-3189; Email: fhuang@zju.edu.cn

Electronic Supporting Information (37 pages)

1. Materials

All reagents including toluene (**Tol**), pyridine (**Py**), 2-methylthiophene (**2-MTP**) and 3-methylthiophene (**3-MTP**) were commercially available and used as supplied without further purification. **EtP6** was synthesized as described previously.[S1] Activated crystalline **EtP6** (**EtP6***β*) was recrystallized from acetone first and dried under vacuum at 140 °C overnight.

Table S1 Physical properties of the four components.[S2,S3]

Component	Boiling Point (°C)	Melting Point (°C)
Tol	110.6	–94.9
Py	115.2	–41.6
2-MTP	113.0	–63.0
3-MTP	114.0	–69.0

2. Methods

2.1 . Solution NMR

Solution ^{1}H NMR spectra were recorded at 400.13 MHz using a Bruker Avance 400 NMR spectrometer.

2.2. Thermogravimetric Analysis

Thermogravimetric Analysis (TGA) was carried out using a Q5000IR analyzer (TA instruments) with an automated vertical overhead thermobalance. The samples were heated at the rate of 10 ℃/min using N_2 as the protective gas.

2.3. Powder X-Ray Diffraction

Powder X-ray diffraction (PXRD) data were collected on a Rigaku Ultimate-IV X-ray diffractometer operating at 40 kV/30 Ma using the Cu Kα line (λ = 1.5418 Å). Data were measured over the range of 5–45 °in 5 °/min steps over 8 min.

2.4. Single Crystal Growth

All single crystals of heterocyclic compound-loaded **EtP6** were grown by slow evaporation: 5 mg of dry **EtP6** powder was put in a small vial where 2 mL of a heterocyclic compound was added. The resultant transparent solution was allowed to evaporate slowly to give nice colorless crystals in 5 to 10 days.

2.5. Single Crystal X-Ray Diffraction

Suitable crystals were selected and measured on a Bruker D8 Ventune diffractometer with Mo-Kα radiation (λ = 0.71073 Å) for cell determination and subsequent data collection at 293K. Supplementary CIFs, which include structure factors, are available free of charge from the Cambridge Crystallographic Data Centre (CCDC) via https://www.ccdc.cam.ac.uk/structures/.

2.6. Gas Chromatography

Gas Chromatographic (GC) Analysis: GC measurements were carried out using an Agilent 7890B instrument configured with an FID detector and a DB-624 column (30 m × 0.53 mm × 3.0 μm). Samples were analyzed using headspace injections and were performed by incubating the sample at 80 ℃ for 10 min followed by sampling 1 mL of the headspace. The following GC method was used: the oven was programmed from 50 ℃, and ramped in 10 ℃/min increments to 150 ℃ with 15 min hold; the total run time was 25 min; injection temperature was 250 ℃; detector temperature was 280 ℃ with nitrogen, air, and make-up flow-rates of 35, 350, and 35 mL/min, respectively; helium (carrier gas) flowrate was 3.0 mL/min. The samples were injected in the split mode (30:1).

2.7. Gas Chromatography-Mass Spectrometry

Gas Chromatographic-Mass Spectrometric (GC-MS) analysis was carried out on an HP6890 gas chromatograph instrument with an HP5973 mass spectrometric detector equipped with an electron ionization source and a single-stage quadrupole. Analytes were separated on an HP-wax capillary column, 30 m × 0.25 mm I.D. and 0.25 μm phase thickness. The helium carrier gas was set at a constant flow-rate of 1 mL/min.

Sample injection was done with an HP 7683 autosampler. The 10 μL syringe was washed three times with ethyl acetate before and after each run and rinsed with 8 μL of the sample solution before 1 μL of the sample solution was injected in the split mode. The temperatures of the GC-MS instrument were set at 250 ℃ at the injector and 250 ℃ at the transfer line. The GC oven was maintained at 60 ℃ for 2 min, ramped at a rate of 20 ℃/min to 240 ℃ and held at this temperature for 2 min.

3. Crystallographic Data

Table S2 Experimental single crystal X-ray data for guest-loaded **EtP6** structures.

	$(Py)_2$@EtP6	**$(2\text{-MTP})_3$@EtP6**	**$(3\text{-MTP})_3$@EtP6**
Crystallization Solvent	**Py**	**2-MTP**	**3-MTP**
Collection Temperature	170 K	170 K	170 K
Formula	$C_{82}H_{89}NO_{12}$	$C_{81}H_{100}O_{12}S_3$	$C_{81}H_{102}O_{12}S_3$
Mr	1280.54	1361.78	1363.80
Crystal Size [mm]	0.05 × 0.03 × 0.01	0.35 × 0.26 × 0.23	0.35 × 0.26 × 0.23
Crystal System	Trigonal	Monoclinic	Monoclinic
Space Group	*P-3*	*C2/c*	*C2/c*
a [Å]	22.4256(13)	27.179(3)	27.421(8)
b [Å]	22.4256(13)	12.5194(12)	12.544(4)
c [Å]	12.5570(10)	25.143(4)	26.222(8)
α [°]			
β [°]		119.830(3)	124.116(9)
γ [°]	120		
V [Å^3]	5469.0(8)	7421.9(15)	7467(4)
Z	3	4	4
D_{calcd} [g cm^{-3}]	1.166	1.219	1.213
μ[mm^{-1}]	0.397	0.161	0.160
F(000)	2052	2920	2928
2θ range [°]	6.124–110.846	4.502–52.846	4.504–56.814
Reflections collected	40179	30205	33476
Independent reflections, R_{int}	7018, 0.1278	7577, 0.0571	8204, 0.0528
Obs. Data [$I > 2\sigma(I)$]	2394	5781	6535
Data / restraints / parameters	7018 / 72 / 571	7577 / 276 / 520	8204 / 185 / 522
Final R_1 values ($I > 2\sigma(I)$)	0.1262	0.1233	0.1311
Final R_1 values (all data)	0.2375	0.1406	0.1461
Final $wR(F_2)$ values (all data)	0.4377	0.3198	0.3516
Goodness-of-fit on F^2	1.102	0.971	0.979
Largest difference peak and hole [e.A^{-3}]	0.298 / –0.285	1.172 / –0.862	0.747 / –0.772
CCDC	1958820	1958824	1958825

*4. Characterization of Desolvated **EtP6** crystals (**EtP6**β)*

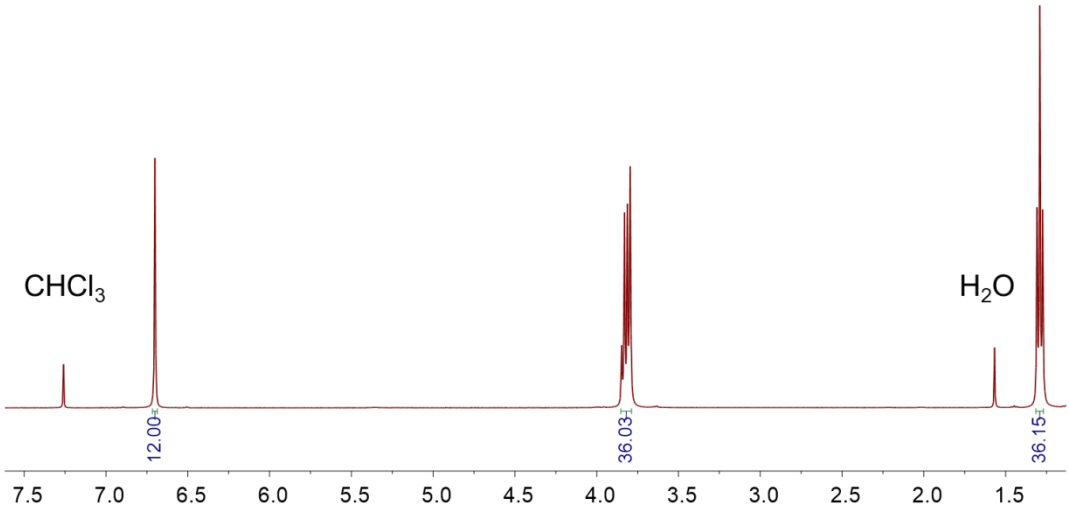

Fig. S1 ^{1}H NMR spectrum (400 MHz, chloroform-*d*, 298 K) of **EtP6**β.

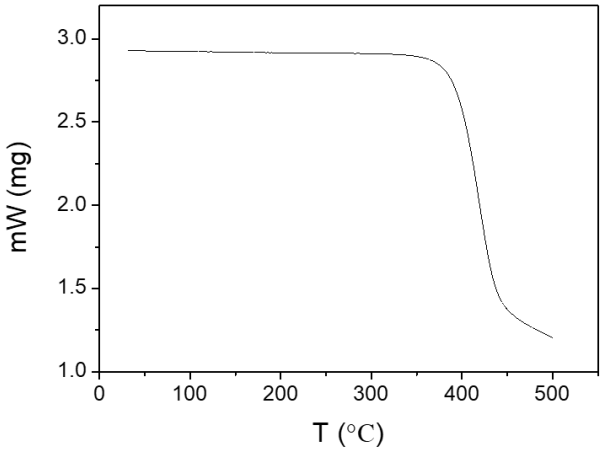

Fig. S2 Thermogravimetric analysis of desolvated **EtP6**β.

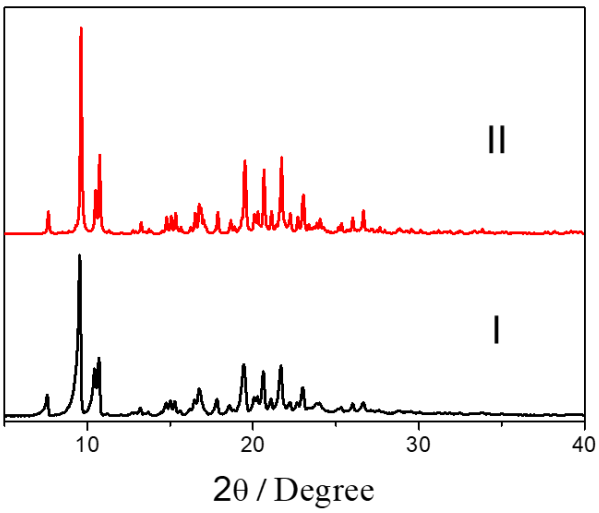

Fig. S3 Powder X-ray diffraction patterns: (I) activated **EtP6** crystals (**EtP6***β*); (II) simulated from single crystal structure of guest-free **EtP6**.[S4]

5. Vapor-Phase Adsorption Measurements

*5.1 Single-Component Adsorption Experiments of **EtP6**β*

For each single-component adsorption experiments, an open 5 mL vial containing 20 mg of the guest-free **EtP6**β adsorbent was placed in a sealed 20 mL vial containing 2 mL of single-component heterocyclic compound liquid. Uptake in the **EtP6**β crystals was measured hour by hour by completely dissolving the crystals and measuring the adsorption ratio of **EtP6** by ^{1}H NMR. Before measurements, the crystals were heated at 30 °C to remove the surface-physically adsorbed vapor molecules.

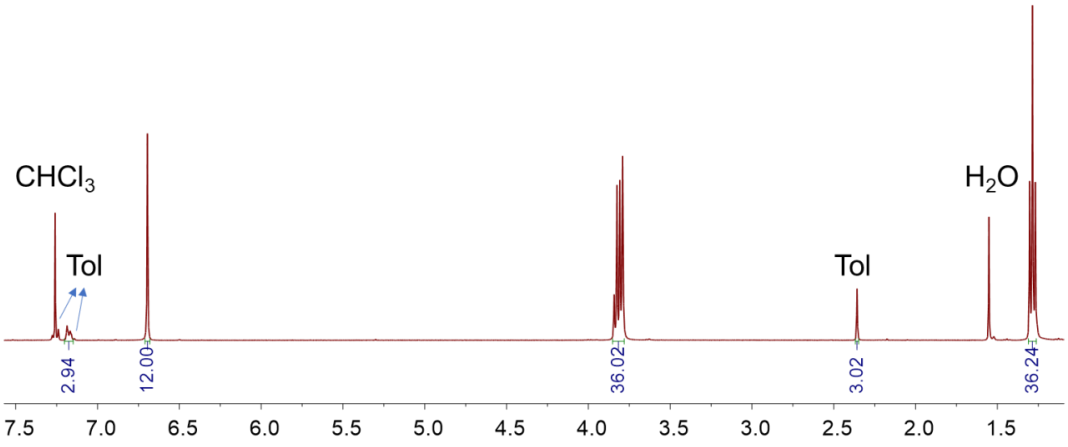

Fig. S4 ^{1}H NMR spectrum (400 MHz, chloroform-*d*, 298 K) of **EtP6**β after sorption of **Tol** vapor.

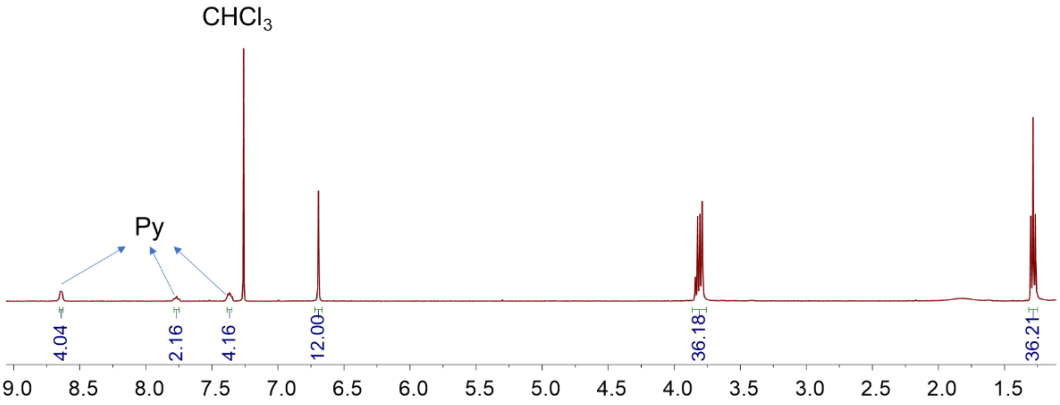

Fig. S5 ^{1}H NMR spectrum (400 MHz, chloroform-*d*, 298 K) of **EtP6***β* after sorption of **Py** vapor.

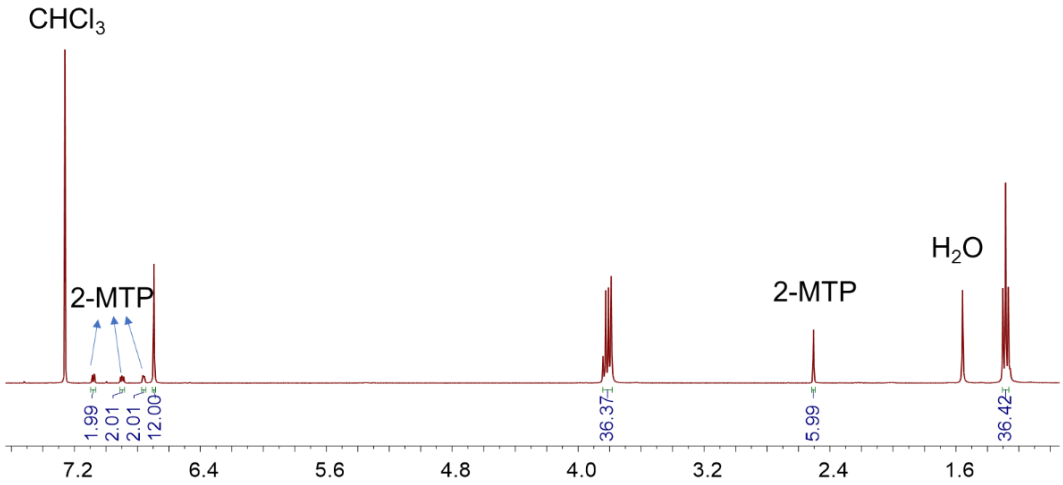

Fig. S6 ^{1}H NMR spectrum (400 MHz, chloroform-*d*, 298 K) of **EtP6***β* after sorption of **2-MTP** vapor.

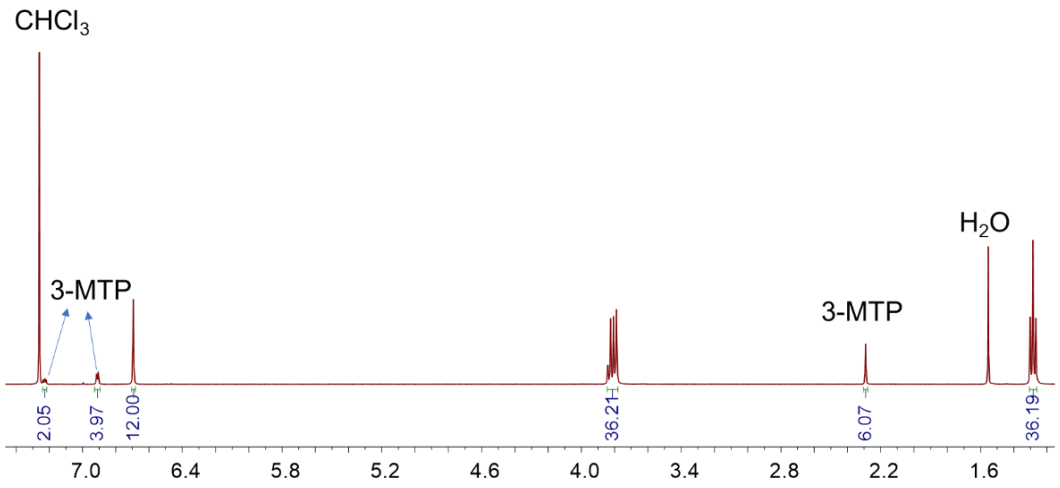

Fig. S7 ^{1}H NMR spectrum (400 MHz, chloroform-*d*, 298 K) of **EtP6*β*** after sorption of **3-MTP** vapor.

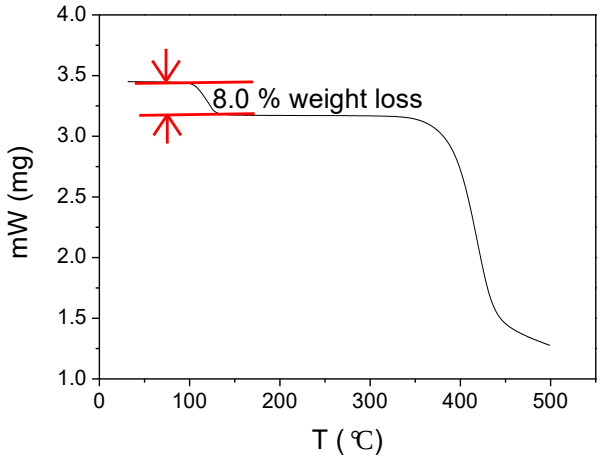

Fig. S8 Thermogravimetric analysis of **EtP6*β*** after adsorption of **Tol**. The weight loss below 150 °C can be calculated as one **Tol** molecule per **EtP6** molecule.

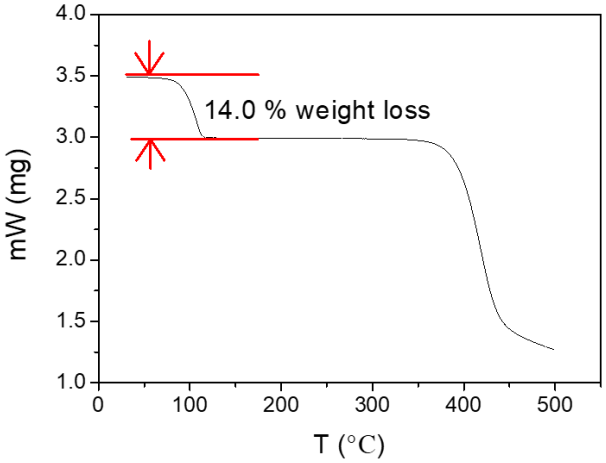

Fig. S9 Thermogravimetric analysis of **EtP6**β after adsorption of **Py**. The weight loss below 150 °C can be calculated as two **Py** molecules per **EtP6** molecule.

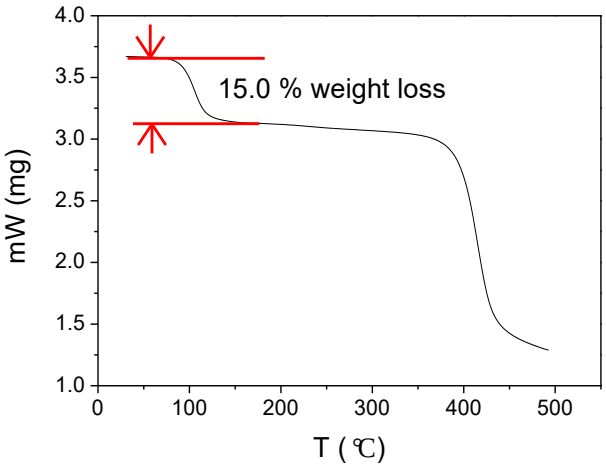

Fig. S10 Thermogravimetric analysis of **EtP6**β after adsorption of **2-MTP**. The weight loss below 150 °C can be calculated as two **2-MTP** molecules per **EtP6** molecule.

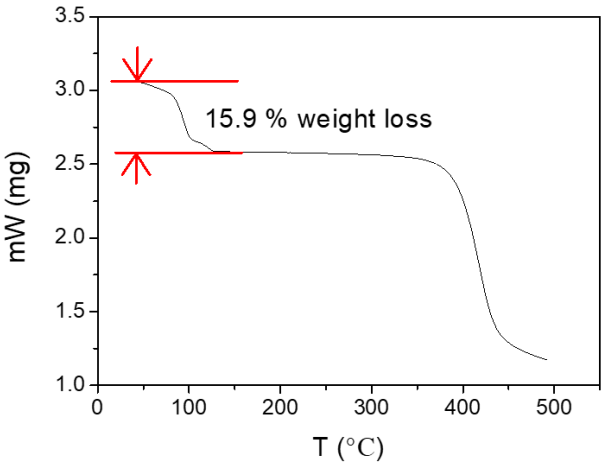

Fig. S11 Thermogravimetric analysis of **EtP6*β*** after adsorption of **3-MTP**. The weight loss below 150 °C can be calculated as two **3-MTP** molecules per **EtP6** molecule.

5.2. Structural Analyses after Single-Component Vapor Sorption

In the crystal structure of **Py**-loaded **EtP6** (**(Py)$_2$@EtP6**), the N atom of the pyridine ring is in the same position as the C atoms, but their occupancy ratios are different. The C atom occupancy ratio is 5/6, and the N atom occupancy ratio is 1/6. Two **Py** molecules located in the cavity of the host are stabilized by π-π stacking interactions.

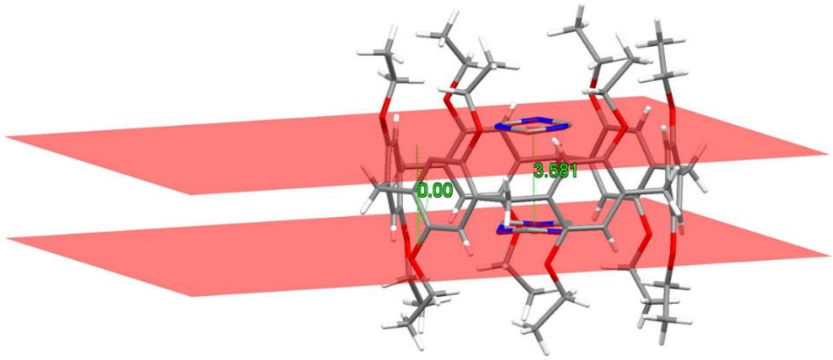

Fig. S12 Single crystal structure of **(Py)$_2$@EtP6**. Ring plane/ring plane inclinations: 0.00 °; centroid–centroid distance (Å): 3.581.

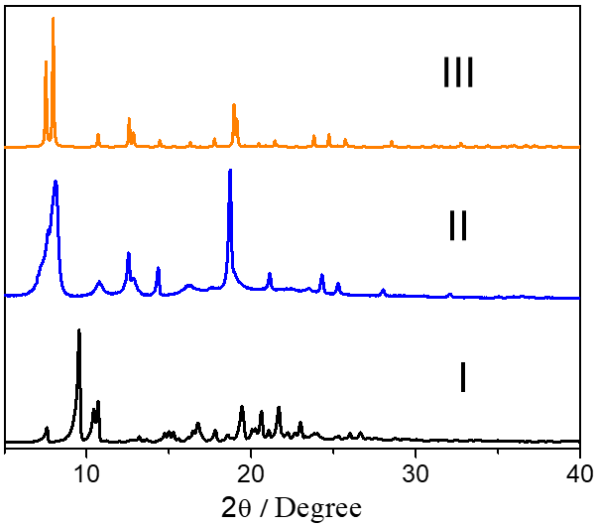

Fig. S13 Powder X-ray diffraction patterns of **EtP6**: (I) **EtP6*β***; (II) **EtP6*β*** after adsorption of **Py**; (III) simulated from the single crystal structure of **(Py)$_2$@EtP6**.

In the crystal structure of **(2-MTP)**-loaded **EtP6** (**(2-MTP)$_3$@EtP6**), two **2-MTP** molecules are located in the cavity of **EtP6**, stabilized by hydrogen bonds. However, another **2-MTP** molecule is located in the channel formed by two adjacent **EtP6** molecules and has negligible interactions with the two hosts.

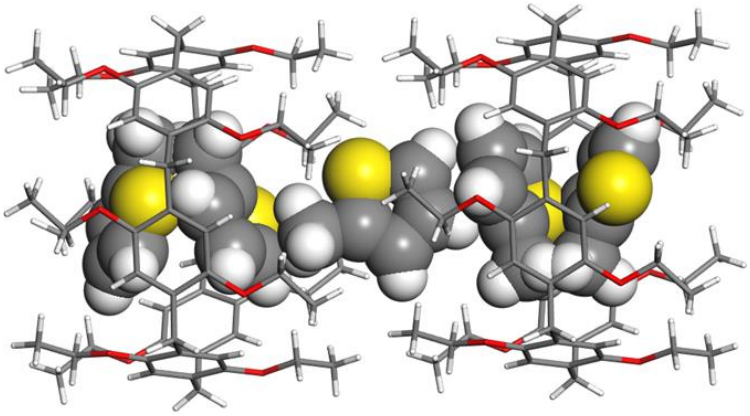

Fig. S14 Single crystal structure of **(2-MTP)$_3$@EtP6** along *a* axis.

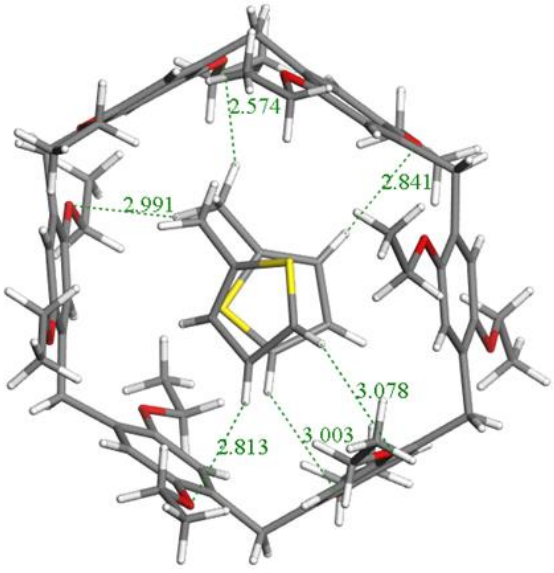

Fig. S15 Single crystal structure of **(2-MTP)$_3$@EtP6**. CH ··O distances (Å): 2.574, 2.813, 2.841, 2.991, 3.003, 3.078.

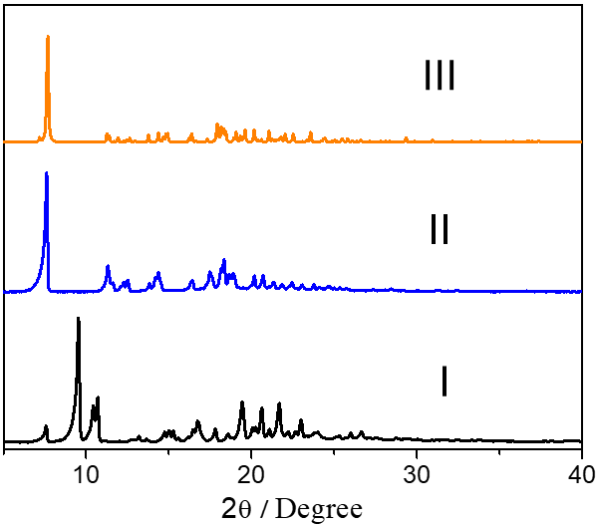

Fig. S16 Powder X-ray diffraction patterns of **EtP6**: (I) **EtP6**β; (II) **EtP6**β after adsorption of **2-MTP**; (III) simulated from the single crystal structure of **(2-MTP)$_3$@EtP6**.

In the crystal structure of **(3-MTP)**-loaded **EtP6** (**(3-MTP)$_3$@EtP6**), two **3-MTP** molecules are located in the cavity of **EtP6**, stabilized by hydrogen bonds and CH···π interactions. However, another **3-MTP** molecule is located in the channel formed by two adjacent **EtP6** molecules and has negligible interactions with the two hosts.

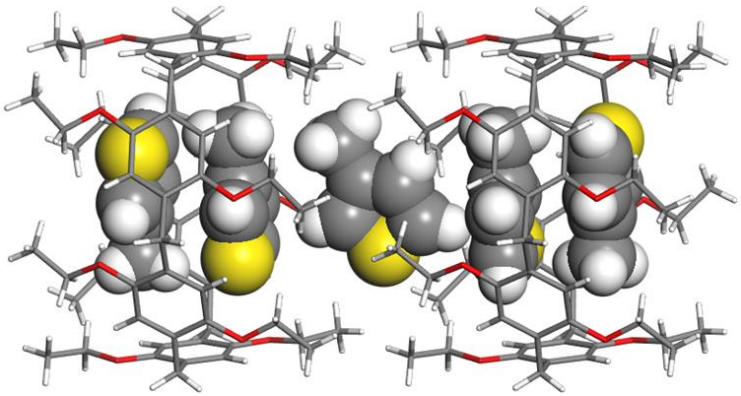

Fig. S17 Single crystal structure of **(3-MTP)$_3$@EtP6** along *a* axis.

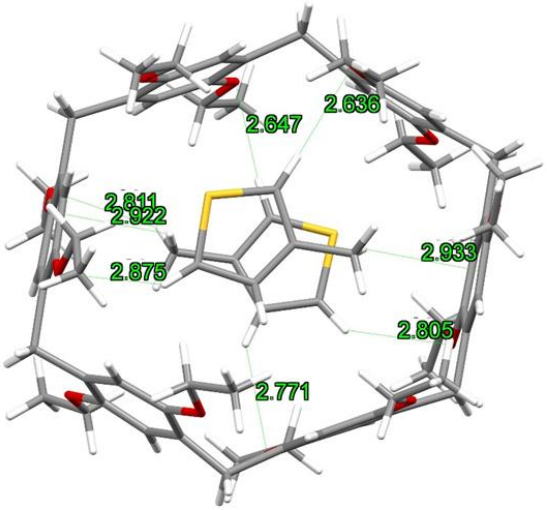

Fig. S18 Single crystal structure of **(3-MTP)$_3$@EtP6**. CH ··O distances (Å): 2.636, 2.647, 2.771, 2.805, 2.811, 2.875; CH···π distances (Å): 2.922, 2.933.

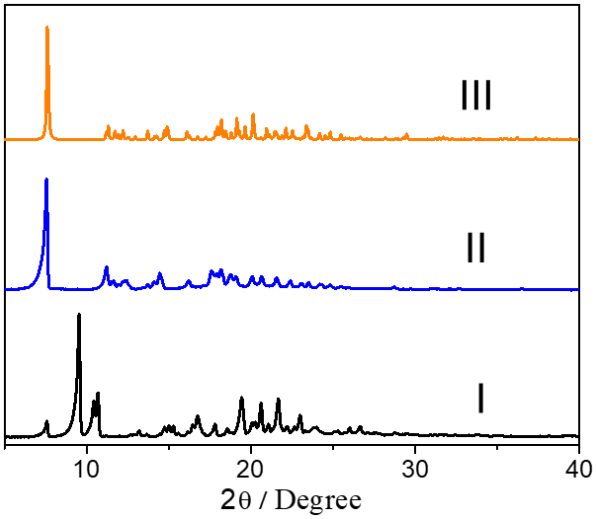

Fig. S19 Powder X-ray diffraction patterns of **EtP6**: (I) **EtP6**β; (II) **EtP6**β after adsorption of **3-MTP**; (III) simulated from the single crystal structure of **(3-MTP)$_3$@EtP6**.

*5.3. Uptake from a Tol/Py Binary Mixture by **EtP6**β*

For each mixture vapor-phase experiment, an open 5 mL vial containing 20 mg of guest-free **EtP6**β adsorbent was placed in a sealed 20 mL vial containing 2 mL of a **Tol**/**Py** mixture (*v*:*v* = 1:1). Uptake in the **EtP6**β crystals was measured hour by hour by completely dissolving the crystals and measuring the ratio of **Tol** or **Py** to **EtP6** by ^{1}H NMR. The relative uptake of **Tol** or **Py** in **EtP6**β was also measured by heating the crystals to release the adsorbed vapor using gas chromatography. Before measurements, the crystals were heated at 30 °C to remove the surface-physically adsorbed guest molecules.

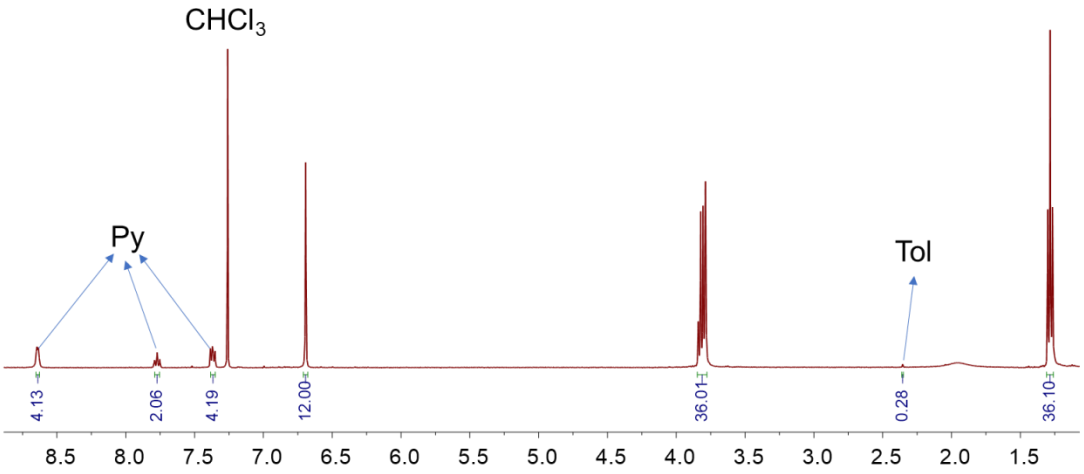

Fig. S20 ^{1}H NMR spectrum (400 MHz, chloroform-*d*, 298 K) of **EtP6**β after sorption of **Tol**/**Py** mixture vapor.

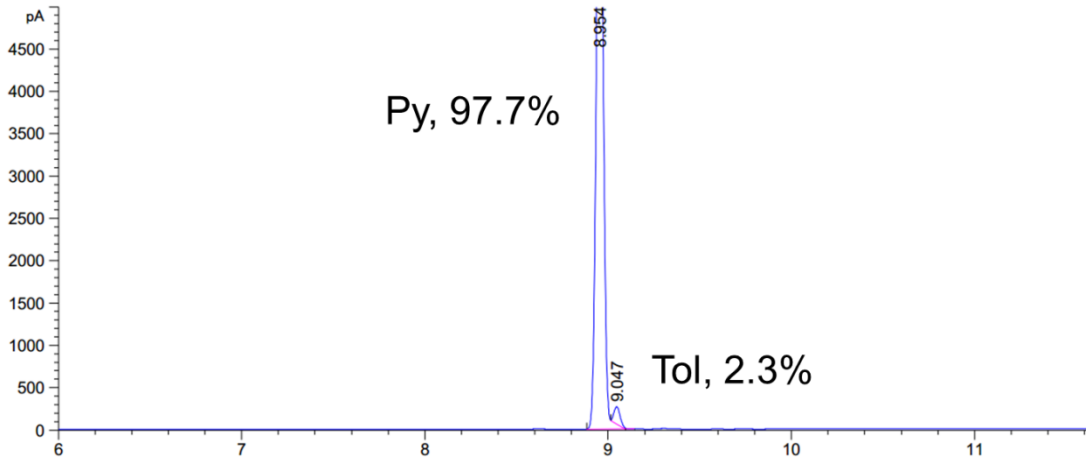

Fig. S21 Relative uptakes of **Tol** and **Py** adsorbed in **EtP6***β* based on gas chromatography after 12 hour vapor adsorption of a **Tol**/**Py** mixture (*v*:*v* = 1:1).

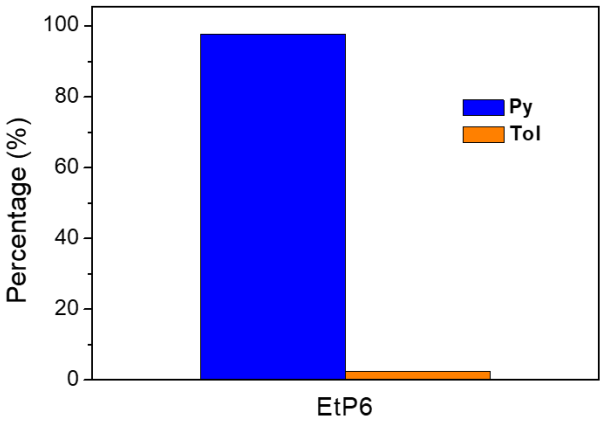

Fig. S22 Relative amounts of **Tol** and **Py** adsorbed by **EtP6***β* over 12 hours as measured by gas chromatography.

For a mixture of **Tol** and **Py**, **EtP6**β can selectively capture **Py** vapor, resulting in a structural transformation from guest-free **EtP6** to **(Py)**$_2$**@EtP6**. In addition, the loaded guest molecules can be removed by heating at 100 °C, thereby obtaining 97.7% purity **Py**.

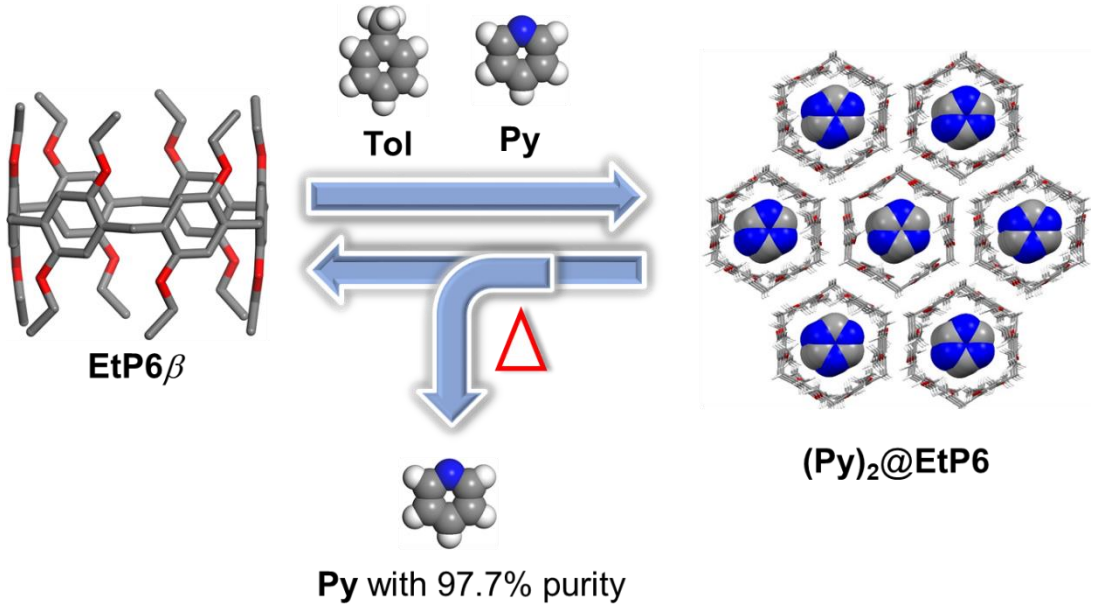

Fig. S23 Structural representation of the transformation from **EtP6**β to **(Py)**$_2$**@EtP6** upon uptake of **Tol**/**Py** mixture vapor and the release of **Py** by heating.

*5.4. Uptake from a **Tol/2-MTP** Binary Mixture by **EtP6**β*

For each mixture vapor-phase experiment, an open 5 mL vial containing 20 mg of guest-free **EtP6**β adsorbent was placed in a sealed 20 mL vial containing 2 mL of a **Tol**/**2-MTP** mixture (*v*:*v* = 1:1). Uptake in the **EtP6**β crystals was measured hour by hour by completely dissolving the crystals and measuring the ratio of **Tol** or **2-MTP** to **EtP6** by ^{1}H NMR. The relative uptake of **Tol** or **2-MTP** in **EtP6**β was also measured by heating the crystals to release the adsorbed vapor using gas chromatography. Before measurements, the crystals were heated at 30 °C to remove the surface-physically adsorbed guest molecules.

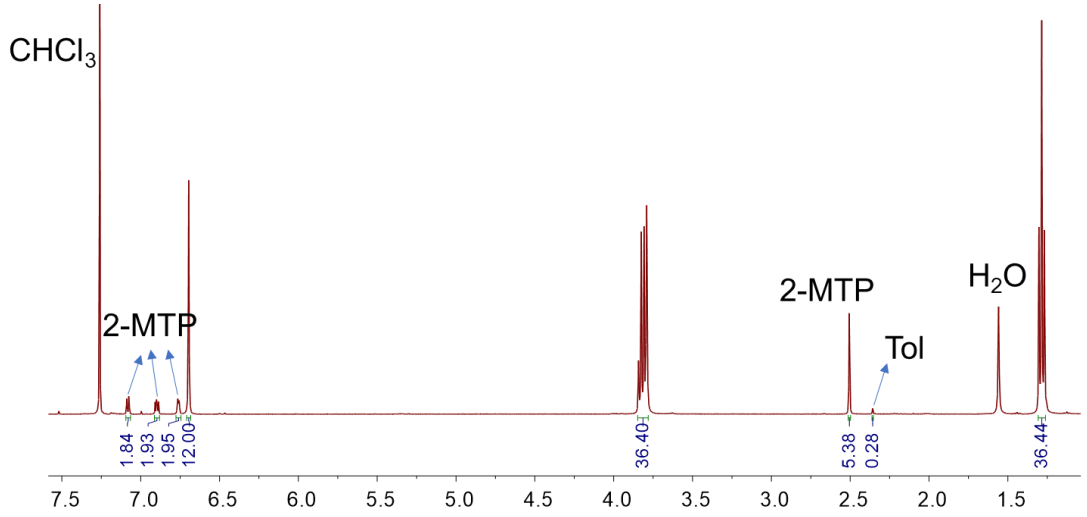

Fig. S24 ^{1}H NMR spectrum (400 MHz, chloroform-*d*, 298 K) of **EtP6**β after sorption of **Tol**/**2-MTP** mixture vapor.

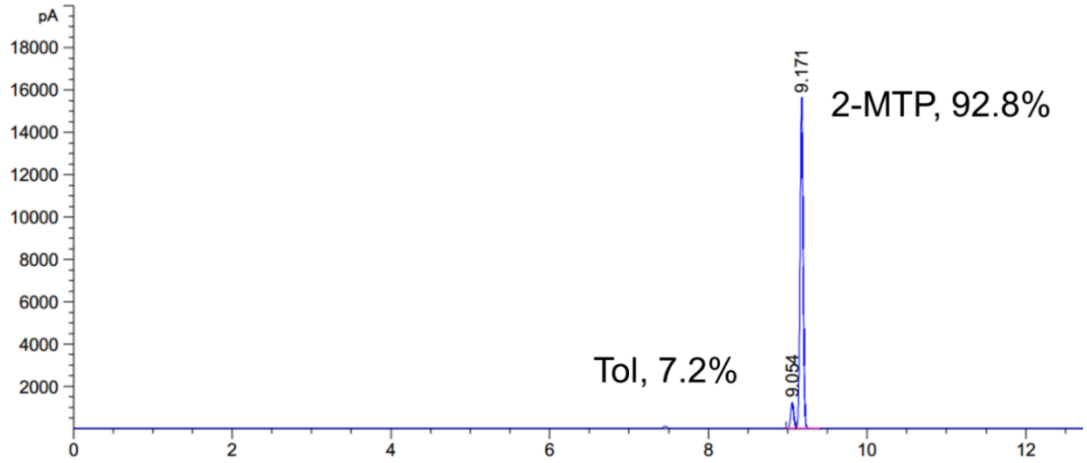

Fig. S25 Relative uptakes of **Tol** and **2-MTP** adsorbed in **EtP6*β*** based on gas chromatography after 12 hour vapor adsorption of a **Tol**/**2-MTP** mixture (*v*:*v* = 1:1)

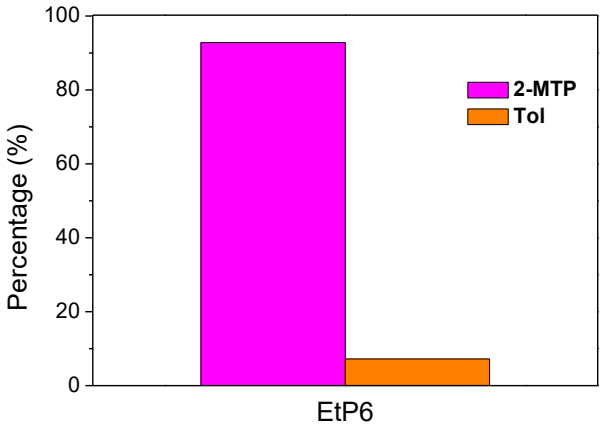

Fig. S26 Relative amounts of **Tol** and **2-MTP** adsorbed by **EtP6*β*** over 12 hours as measured by gas chromatography.

For a mixture of **Tol** and **2-MTP**, **EtP6**β can selectively capture **2-MTP** vapor, resulting in a structural transformation from guest-free **EtP6** to **(2-MTP)$_3$@EtP6**. In addition, the loaded guest molecules can be removed by heating at 100 °C, thereby obtaining 92.8% purity **2-MTP**.

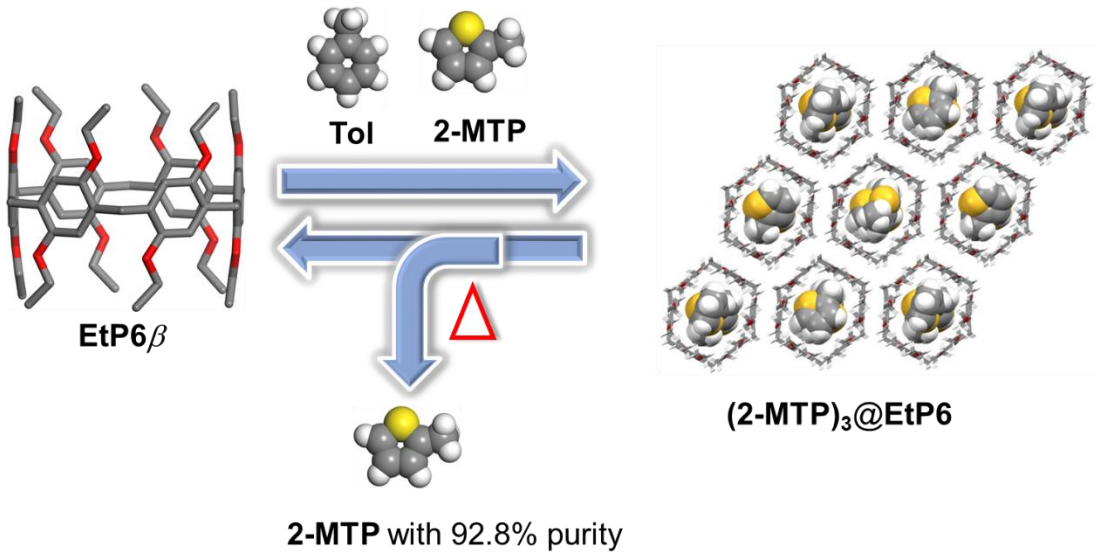

Fig. S27 Structural representation of the transformation from **EtP6**β to **(2-MTP)$_3$@EtP6** upon uptake of **Tol/2-MTP** mixture vapor and the release of **2-MTP** by heating.

*5.5. Uptake from a **Tol/3-MTP** Binary Mixture by **EtP6**β*

For each mixture vapor-phase experiment, an open 5 mL vial containing 20 mg of guest-free **EtP6**β adsorbent was placed in a sealed 20 mL vial containing 2 mL of a **Tol**/**3-MTP** mixture (*v*:*v* = 1:1). Uptake in the **EtP6**β crystals was measured hour by hour by completely dissolving the crystals and measuring the ratio of **Tol** or **3-MTP** to **EtP6** by ^{1}H NMR. The relative uptake of **Tol** or **3-MTP** in **EtP6**β was also measured by heating the crystals to release the adsorbed vapor using gas chromatography. Before measurements, the crystals were heated at 30 °C to remove the surface-physically adsorbed guest molecules.

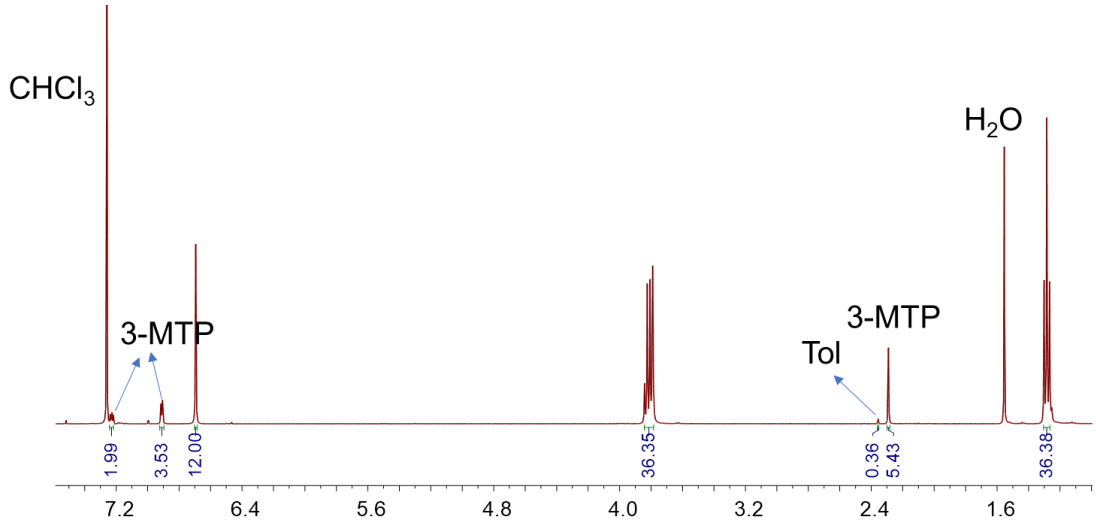

Fig. S28 ^{1}H NMR spectrum (400 MHz, chloroform-*d*, 298 K) of **EtP6**β after sorption of **Tol**/**3-MTP** mixture vapor.

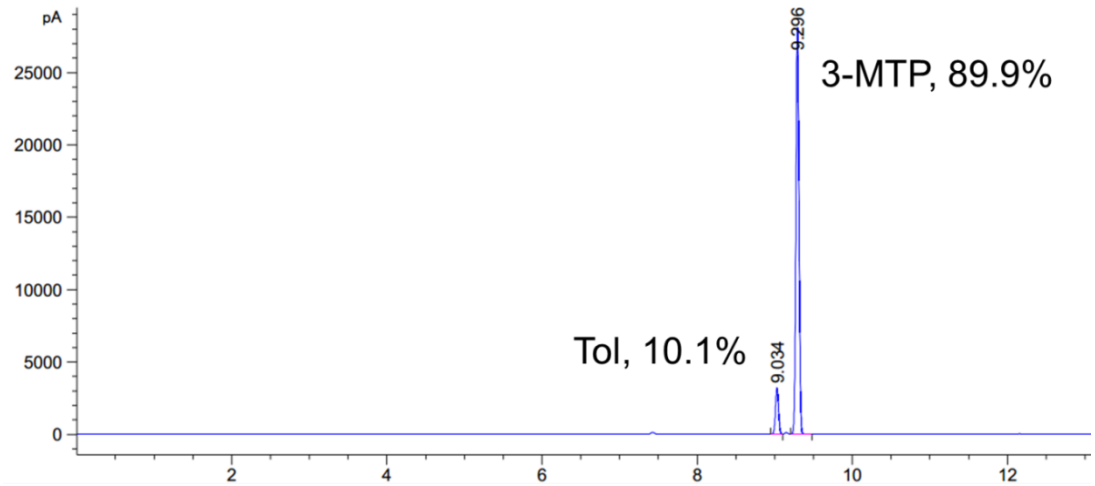

Fig. S29 Relative uptakes of **Tol** and **3-MTP** adsorbed in **EtP6*β*** based on gas chromatography after 12 hour vapor adsorption of a **Tol**/**3-MTP** mixture (*v*:*v* = 1:1)

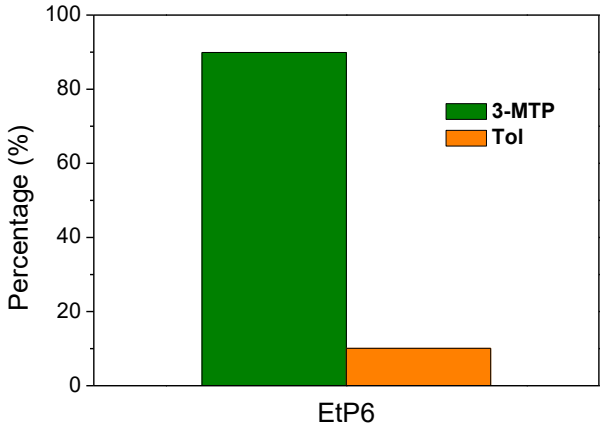

Fig. S30 Relative amounts of **Tol** and **3-MTP** adsorbed by **EtP6*β*** over 12 hours as measured by gas chromatography.

For a mixture of **Tol** and **3-MTP**, **EtP6**β can selectively capture **3-MTP** vapor, resulting in a structural transformation from guest-free **EtP6** to **(3-MTP)$_3$@EtP6**. In addition, the loaded guest molecules can be removed by heating at 100 °C, thereby obtaining 89.9% purity **3-MTP**.

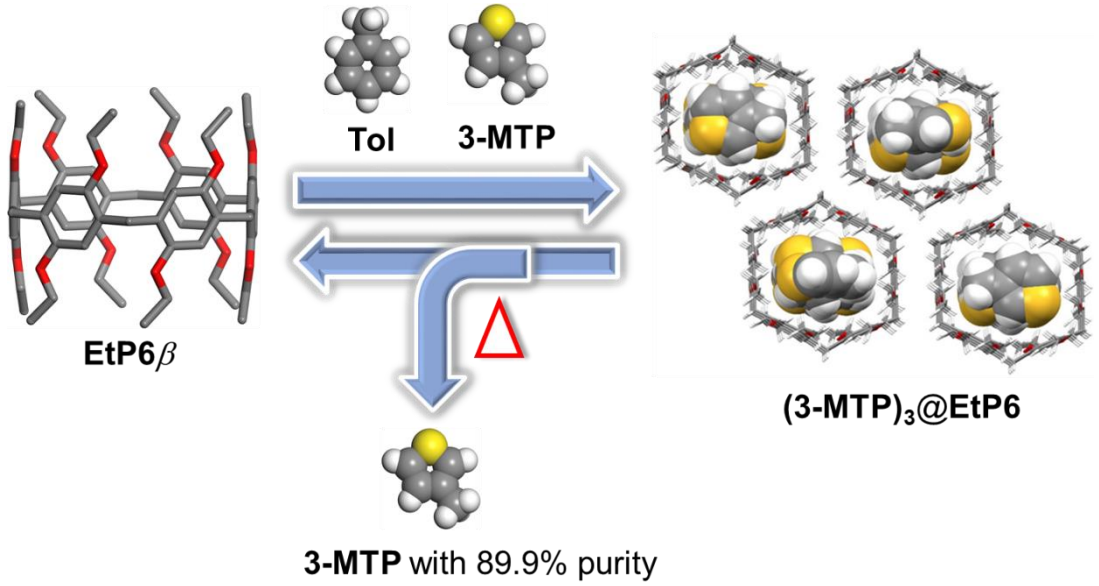

Fig. S31 Structural representation of the transformation from **EtP6**β to **(3-MTP)$_3$@EtP6** upon uptake of **Tol/3-MTP** mixture vapor and the release of **3-MTP** by heating.

*6. Recyclability of **EtP6**β Crystals*

An open 5 mL vial containing 20 mg of **(Py)$_2$@EtP6** was desolvated under vacuum at 100 °C overnight. The resultant crystals were characterized by TGA, PXRD and ^{1}H NMR.

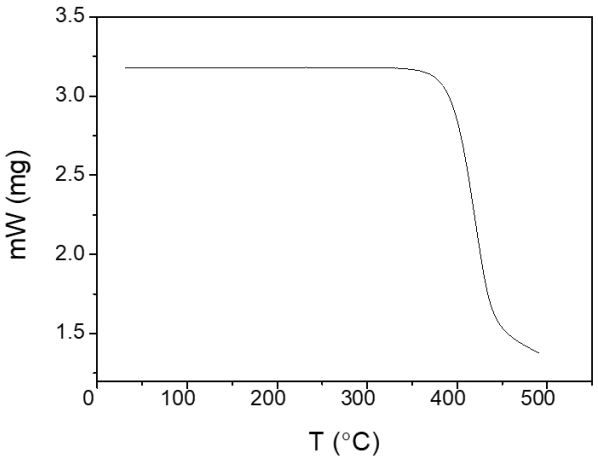

Fig. S32 Thermogravimetric analysis of desolvated **(Py)$_2$@EtP6** upon removal of **Py**.

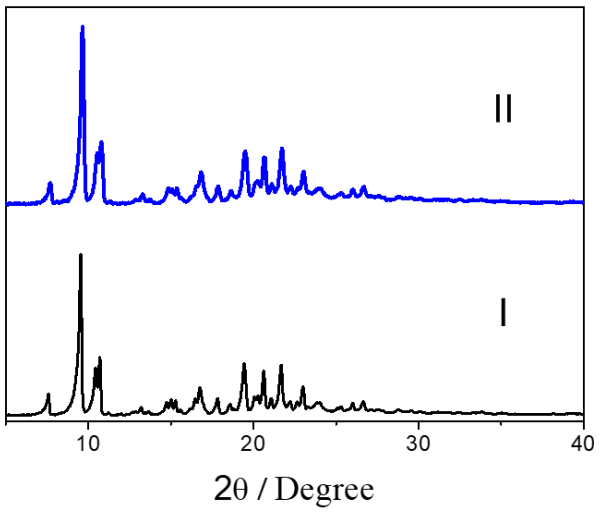

Fig. S33 Powder X-ray diffraction patterns of **EtP6**: (I) **EtP6***β*; (II) desolvated **(Py)$_2$@EtP6**. This shows that upon removal of **Py**, **(Py)$_2$@EtP6** transforms back to **EtP6***β*.

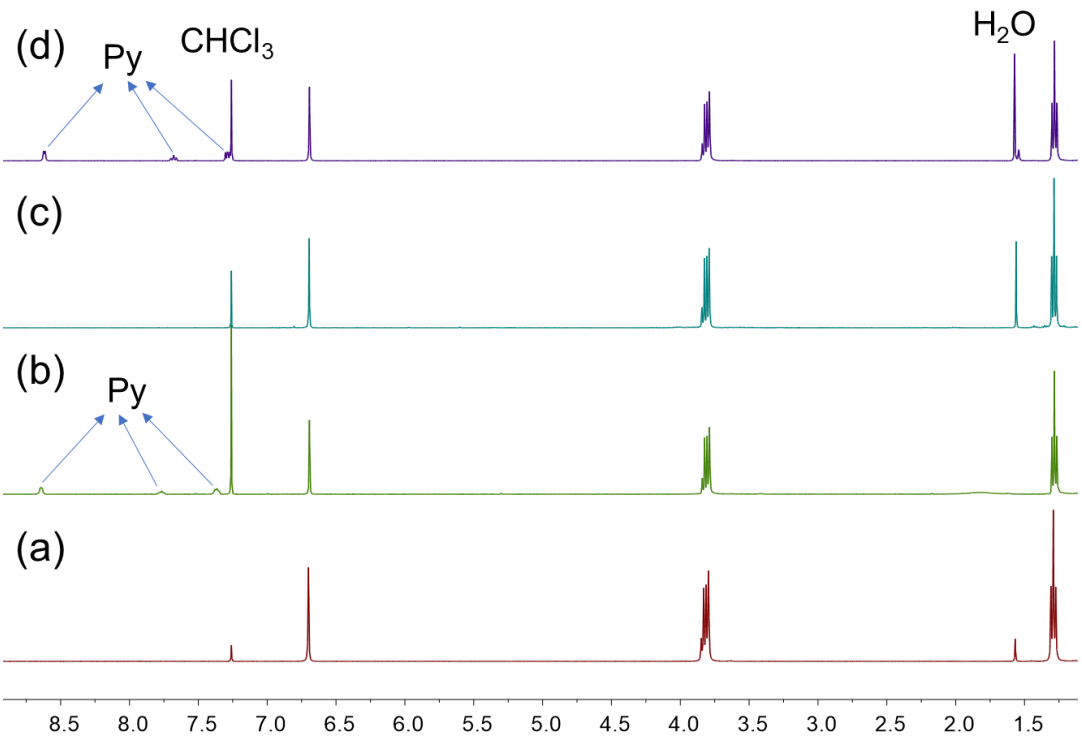

Fig. S34 ^{1}H NMR spectra (400 MHz, chloroform-*d*, 298 K): (a) original **EtP6***β*; (b) **EtP6***β* after adsorption of **Py** vapor; (c) **(Py)$_2$@EtP6** after removal of **Py**; (d) desolvated **(Py)$_2$@EtP6** after adsorption of **Py** vapor.

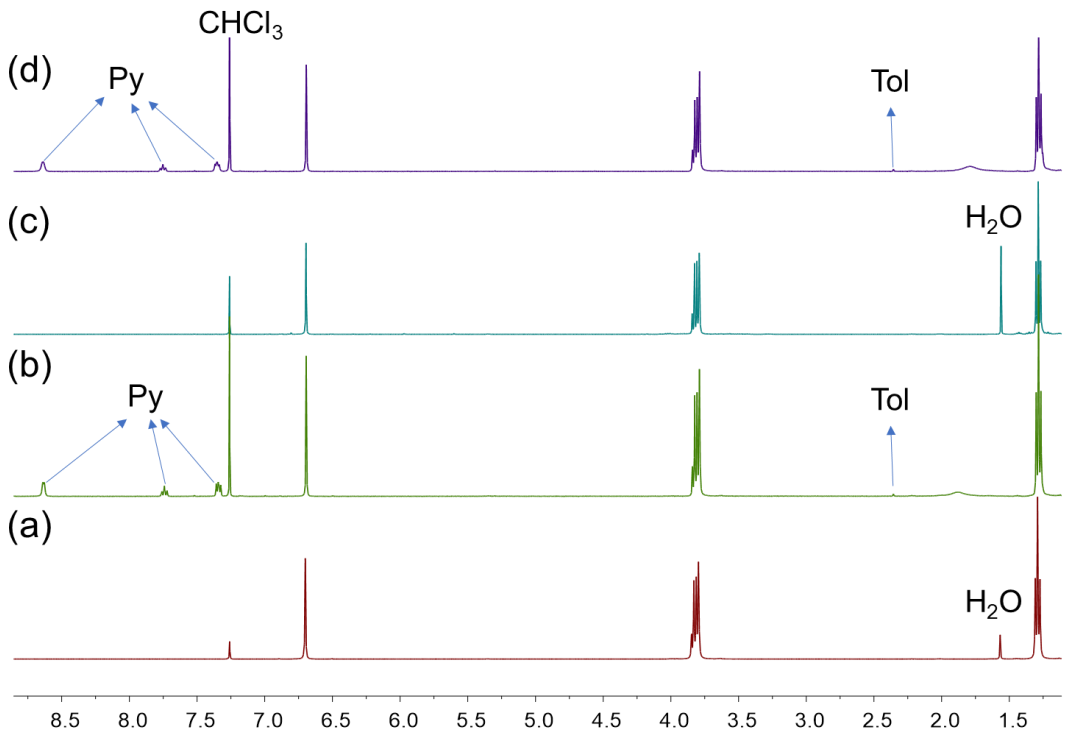

Fig. S35 ^{1}H NMR spectra (400 MHz, chloroform-*d*, 298 K): (a) original **EtP6***β*; (b) **EtP6***β* after adsorption of **Tol/Py** vapor; (c) guest-loaded **EtP6** after removal of **Tol** and **Py**; (d) desolvated guest-loaded **EtP6** after adsorption of **Tol/Py** vapor.

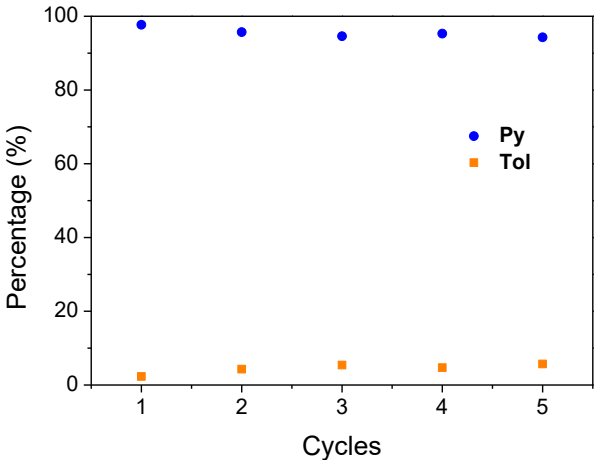

Fig. S36 Relative uptake of **Tol** and **Py** by **EtP6***β* for 12 hours after five recycles.

An open 5 mL vial containing 20 mg of **(2-MTP)$_3$@EtP6** was desolvated under vacuum at 100 °C overnight. The resultant crystals were characterized by TGA, PXRD and ^{1}H NMR.

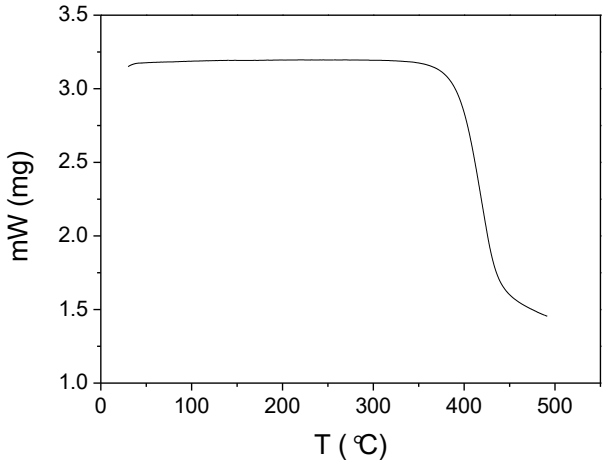

Fig. S37 Thermogravimetric analysis of desolvated **(2-MTP)$_3$@EtP6** upon removal of **2-MTP**.

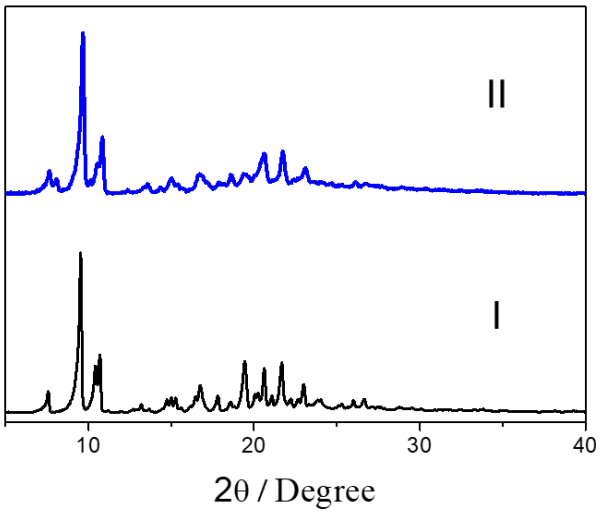

Fig. S38 Powder X-ray diffraction patterns of **EtP6**: (I) **EtP6*β***; (II) desolvated **(2-MTP)$_3$@EtP6**. This shows that upon removal of **2-MTP**, **(2-MTP)$_3$@EtP6** transforms back to **EtP6*β***.

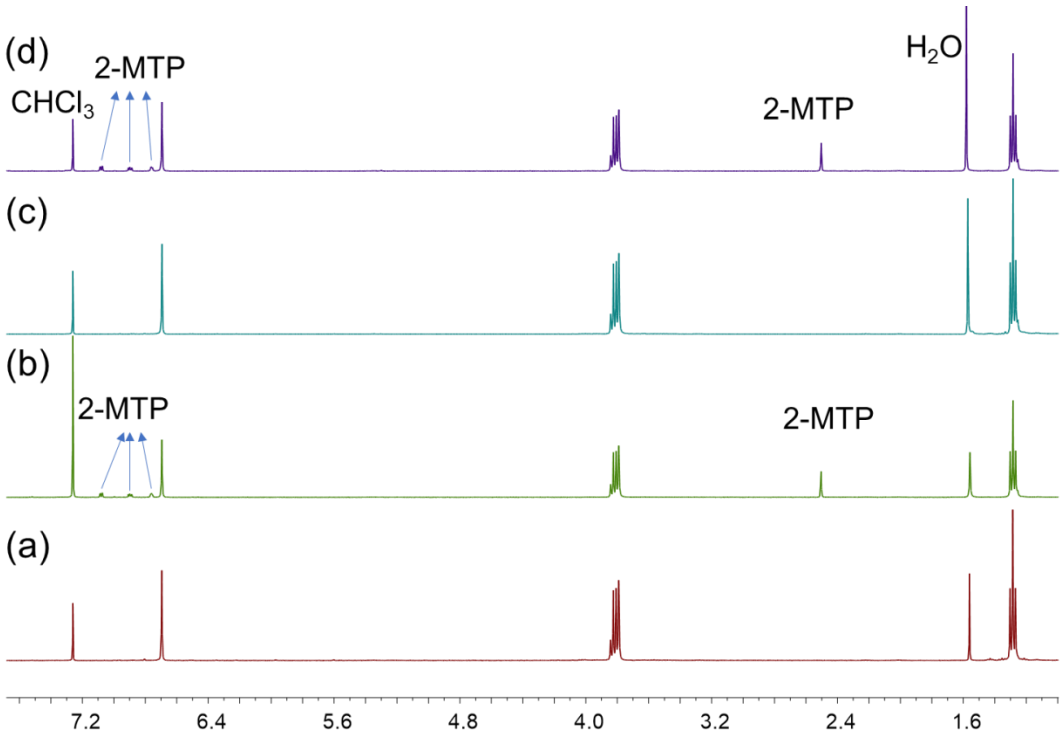

Fig. S39 ^{1}H NMR spectra (400 MHz, chloroform-*d*, 298 K): (a) original **EtP6*β***; (b) **EtP6*β*** after adsorption of **2-MTP** vapor; (c) **(2-MTP)$_3$@EtP6** after removal of **2-MTP**; (d) desolvated **(2-MTP)$_3$@EtP6** after adsorption of **2-MTP** vapor.

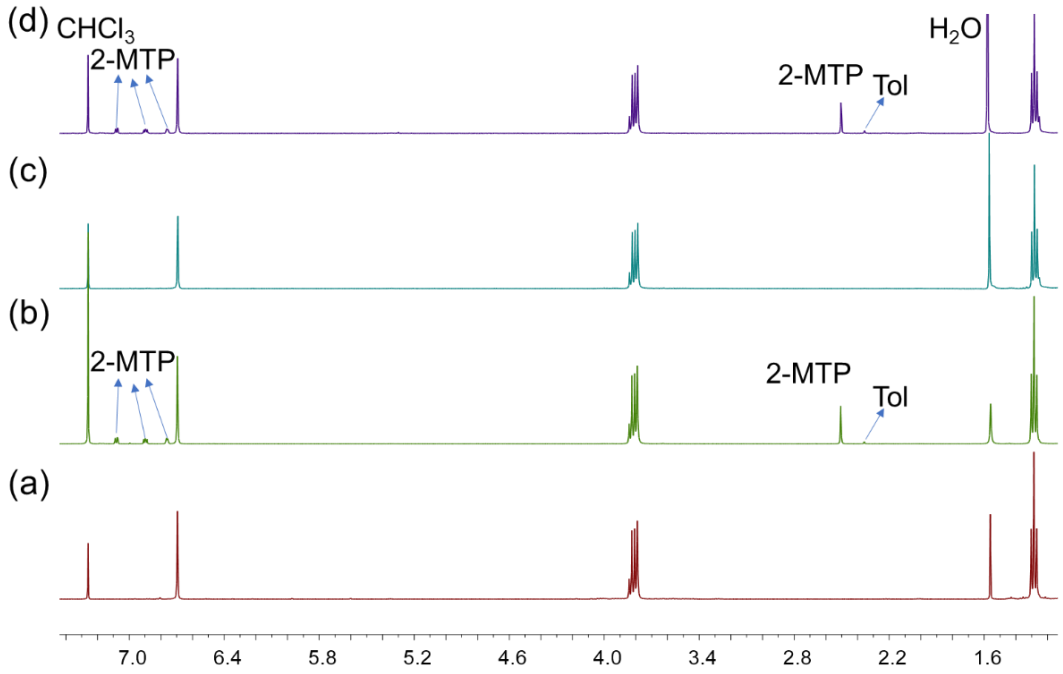

Fig. S40 ^{1}H NMR spectra (400 MHz, chloroform-*d*, 298 K): (a) original **EtP6***β*; (b) **EtP6***β* after adsorption of **Tol/2-MTP** vapor; (c) guest-loaded **EtP6** after removal of **Tol** and **2-MTP**; (d) desolvated guest-loaded **EtP6** after adsorption of **Tol/2-MTP** vapor.

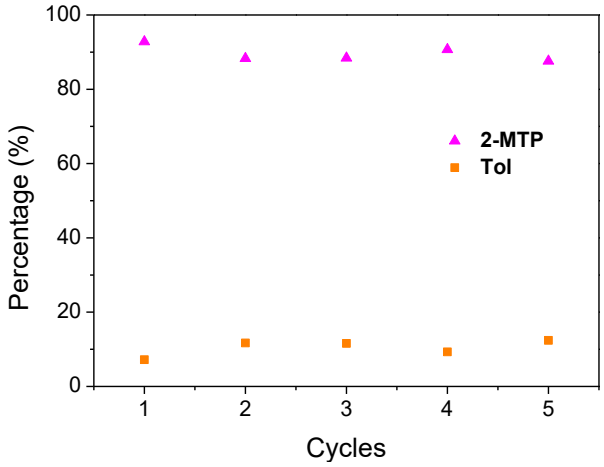

Fig. S41 Relative uptake of **Tol** and **2-MTP** by **EtP6***β* for 12 hours after five recycles.

An open 5 mL vial containing 20 mg of **(3-MTP)$_3$@EtP6** was desolvated under vacuum at 100 °C overnight. The resultant crystals were characterized by TGA, PXRD and ^{1}H NMR.

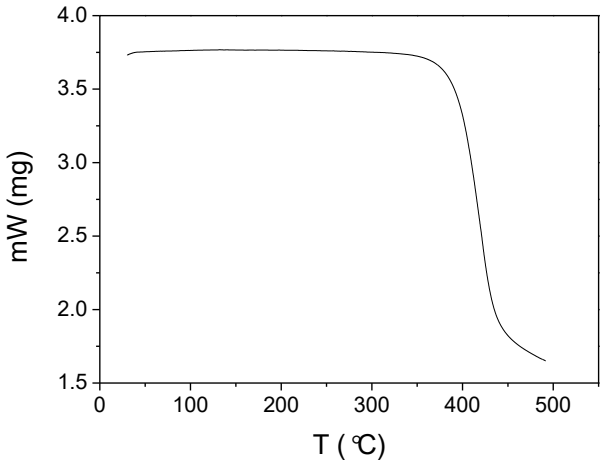

Fig. S42 Thermogravimetric analysis of desolvated **(3-MTP)$_3$@EtP6** upon removal of **3-MTP**.

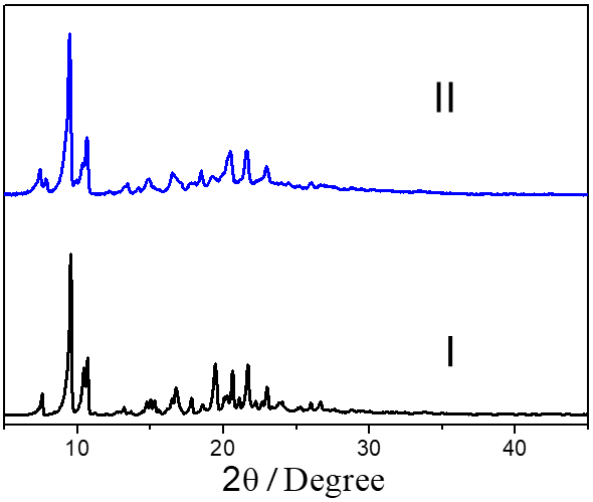

Fig. S43 Powder X-ray diffraction patterns of **EtP6**: (I) **EtP6*β***; (II) desolvated **(3-MTP)$_3$@EtP6**. This shows that upon removal of **3-MTP**, **(3-MTP)$_3$@EtP6** transforms back to **EtP6*β***.

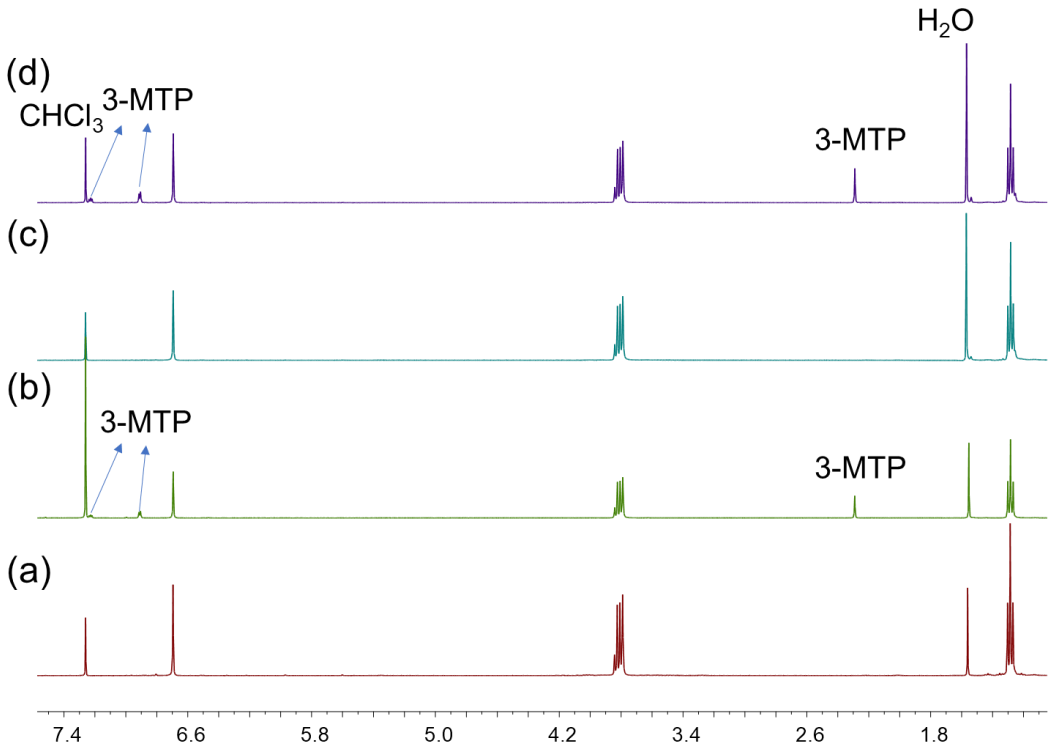

Fig. S44 ^{1}H NMR spectra (400 MHz, chloroform-*d*, 298 K): (a) original **EtP6*β***; (b) **EtP6*β*** after adsorption of **3-MTP** vapor; (c) **(3-MTP)$_3$@EtP6** after removal of **3-MTP**; (d) desolvated **(3-MTP)$_3$@EtP6** after adsorption of **3-MTP** vapor.

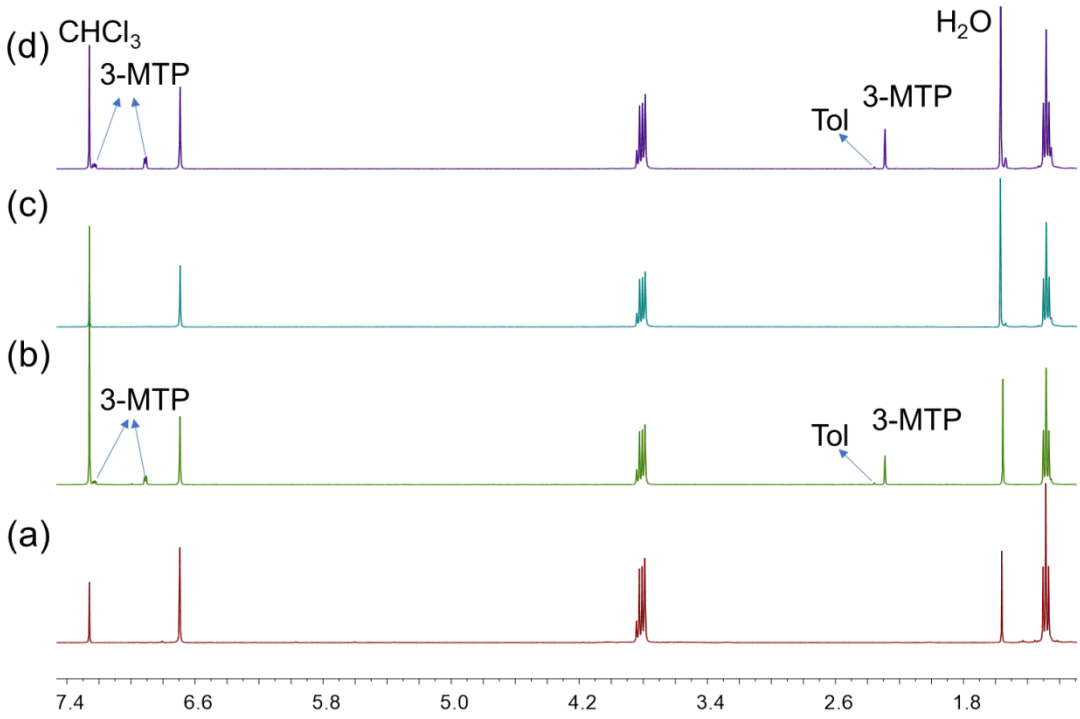

Fig. S45 ^{1}H NMR spectra (400 MHz, chloroform-*d*, 298 K): (a) original **EtP6***β*; (b) **EtP6***β* after adsorption of **Tol/3-MTP** vapor; (c) guest-loaded **EtP6** after removal of **Tol** and **3-MTP**; (d) desolvated guest-loaded **EtP6** after adsorption of **Tol/3-MTP** vapor.

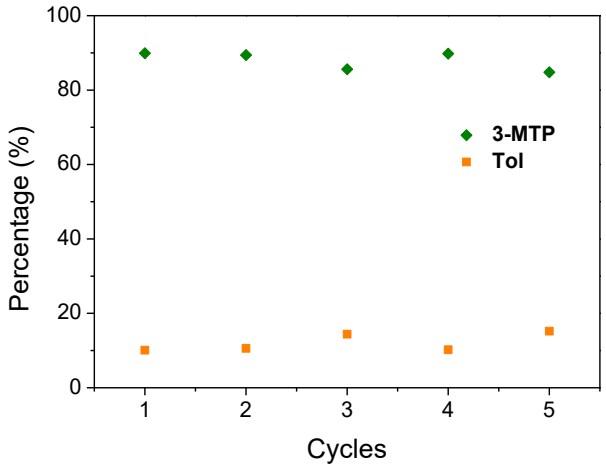

Fig. S46 Relative uptake of **Tol** and **3-MTP** by **EtP6***β* for 12 hours after five recycles.

*7. Toluene Purification by **EtP6**β Crystals*

For the toluene purification experiment, an open 5 mL vial containing 400 mg of the guest-free **EtP6**β adsorbent was placed in a sealed 20 mL vial containing 0.2 mL of a four-component mixture (**Tol/Py/2-MTP/3-MTP**, *v*:*v* = 96.5:1.5:1:1). The purities of toluene before and after adsorption were measured by GC-MS.

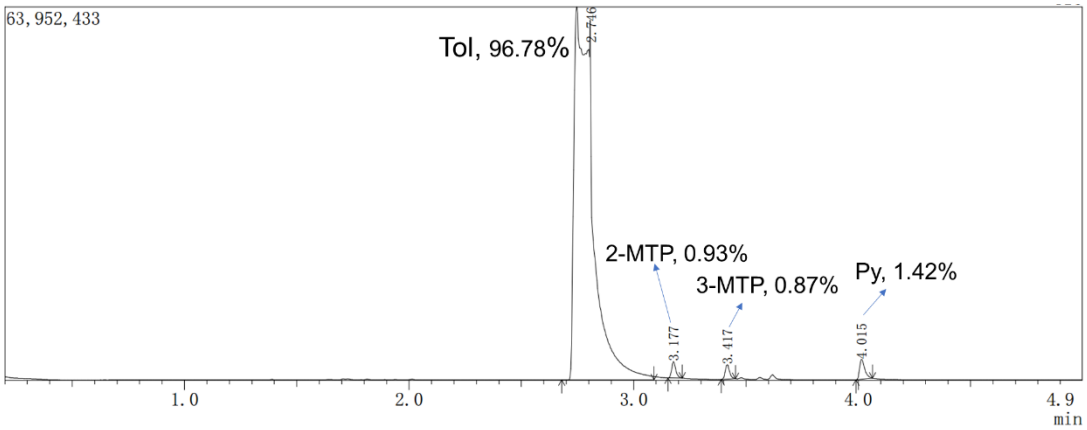

Fig. S47 The purity of **Tol** measured by GC-MS before adsorption.

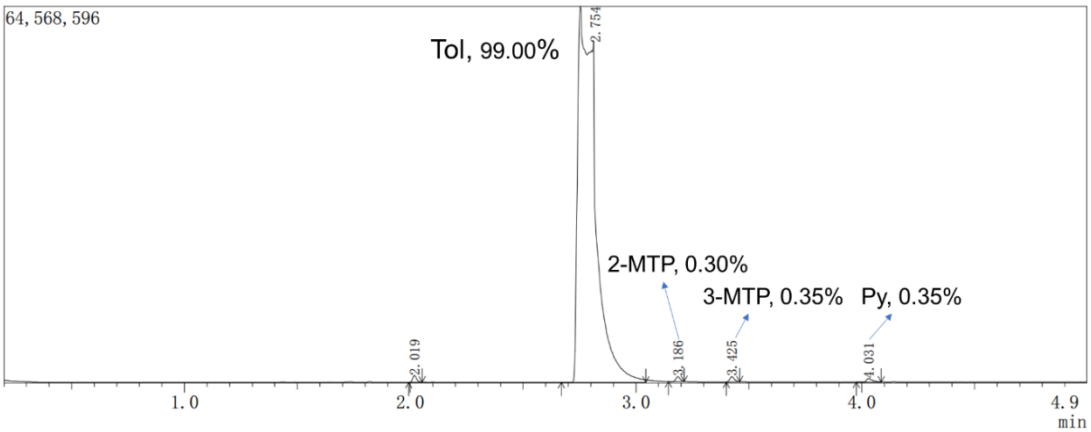

Fig. S48 The purity of **Tol** measured by GC-MS after adsorption.

8. References

S1. X.-B. Hu, Z. Chen, L. Chen, Zhang, L.; J.-L. Hou and Z.-T. Li, Pillar[*n*]arenes (*n* = 8–10) with two Cavities: synthesis, structures and complexing properties, *Chem. Commun.*, 2012, **48**, 10999–11001.

S2. P. Setasuwon, L. Menbangpung and S. Sahasithiwat, Eight combinatorial stacks of three layers of carbon Black/PVA-Carbon Black/EVA composite as a vapor detector array, *J. Comb. Chem.*, 2008, **10**, 959–965.

S3. D. R. Lide, *CRC Handbook of Chemistry and Physics*, Boca Raton, FL, 2005, pp. 3-150.

S4. K. Jie, M. Liu, Y. Zhou, M. A. Little, A. Pulido, S. Y. Chong, A. Stephenson, A. R. Hughes, F. Sakakibara, T. Ogoshi, F. Blanc, G. M. Day, F. Huang and A. I. Cooper, Near-ideal xylene selectivity in adaptive molecular pillar[*n*]arene crystals, *J. Am. Chem. Soc.*, 2018, **140**, 6921–6930.